Molecular Dynamics Simulations of 1,2-Dimethoxyethane/Water Solutions. 1. Conformational and Structural Properties

Dmitry Bedrov, Oleg Borodin, and Grant D. Smith*

Department of Chemical and Fuels Engineering and Department of Materials Science and Engineering, University of Utah, Salt Lake City, Utah 84112

Received: February 4, 1998; In Final Form: April 8, 1998

Molecular dynamics simulations of solutions of 1,2-dimethoxyethane (DME) and water have been performed in order to investigate the conformations of DME and the local solution structure as a function of solution composition and temperature. The simulations employ a previously developed force field based upon ab initio quantum chemistry calculations of DME/water interactions. The DME conformer populations show a strong dependence on temperature and solution composition and are quite different in aqueous solutions from those found in the gas phase or neat liquid. An analysis of the dependence of the conformer population distribution on temperature allows us to estimate the relative free energies of solvation for different conformers in water solution, which are found to be primarily energetic in origin for dilute solutions. The conformation dependence of the solvation free energy, resulting in "hydrophilic" and "hydrophobic" conformers, is explained in terms of differences in polar interactions between DME and neighboring water molecules. Analysis of the local structure of water around different DME conformers reveals that the degree of DME/water hydrogen bonding is nearly independent of the DME conformer for dilute solutions. The extent of water/water hydrogen bonding is also found to be nearly independent of composition over a wide composition range. To maintain a nearly constant level of water−water hydrogen bonding with increasing DME concentration, water is not randomly distributed in the system on a nearest-neighbor length scale but rather tends to form clusters of 4−5 molecules. The entropic penalty associated with this water structure increases with increasing DME concentration and temperature, thereby increasing the free energy of hydrophilic conformers relative to hydrophobic conformers.

I. Introduction

The aqueous solution properties of large ether molecules such as crown ethers and poly(ethylene oxide) (PEO) are of great interest for a wide variety of applications. To gain a better understanding of the interaction of ethers with water and the influence of water on the conformational properties of hydrogen-bond-forming flexible molecules, we have undertaken detailed molecular dynamics simulation studies of 1,2-dimethoxyethane (DME) in aqueous solution. DME, which can be considered the shortest ether molecule to exhibit the local conformational properties of PEO, is illustrated in Figure 1.

In our previous work[1] we developed an atomistic description of DME/water interactions. This molecular mechanics force field was parametrized to reproduce the geometries and energies of DME/water clusters determined from high-level ab initio calculations, while employing an earlier quantum chemistry based force field for DME[2] and the TIP4P (four-point transferable intermolecular potential) model for water.[3] Molecular dynamics simulations of DME in aqueous solution were also performed as a function of solution composition. Thermodynamic properties of the solutions were found to be in excellent agreement with experiment.[1]

In this work we report on the conformational and structural properties of DME/water solutions as a function of concentration and temperature from molecular dynamics simulations using our quantum chemistry based force field. We begin with a brief review of experiments, theory, and previous simulations (including our own work) of DME/water solutions in section II. We also discuss our simulation methodology. In section III we discuss the conformational properties of DME in water. In section IV we consider local structure in DME/water solutions. We make comparisons of simulation predictions with experimental data and theory wherever the latter are available. Finally, in section V we present our conclusions. In an upcoming paper we will discuss the dynamics of DME/water solutions.

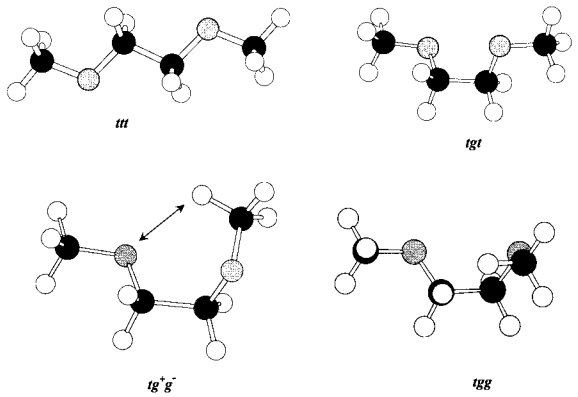

Figure 1. Low-energy conformers of 1,2-dimethoxyethane (DME). The attractive 1,5 $C(H_3)-O$ interaction is indicated.

II. Theory, Experiment, and Previous Simulations

Theory. There are a several theoretical models that attempt to describe the existence of a solubility gap in PEO/water systems by considering (supposed) features of local structure

S1089-5647(98)01009-8 CCC: $15.00
Published on Web 06/17/1998

in the solutions. One model proposed by Kjellander and Florin[4] assumes that PEO is easily accommodated into the liquid water network, resulting in favorable enthalpic interactions between the ether and water. However, the hydrophobic hydration of the methylene (or methyl units) results in increased water structure that is entropically unfavorable. This low-entropy structure results in phase separation at elevated temperatures. As the temperature is increased even more, entropy of mixing results in miscibility. Alternative models,[5,6] which emphasize differences in interactions between "hydrophilic" and "hydrophobic" regions of the polymer chain with water, have been proposed. The models suggest that the intermolecular potential between the two types of molecules forming a solubility gap (water and PEO) have regions that are strongly attractive and regions that are repulsive toward water. At low temperature, the polymer molecules are primarily in the attractive domain, but at elevated temperatures the population of the repulsive regions increase, resulting in an enthalpically driven phase separation. At even higher temperature, the mixing entropy will dominate, resulting in a miscible system. The physical nature of the difference between attractive and repulsive domains is not clear. Goldstein[5] suggested that this difference is due to the capability of different domains to make greater or fewer hydrogen bonds with surrounded water. Karlstrom[6] assumed that the origin of this classification is differences in polar interactions of various PEO conformers with water. All of these Flory−Huggins-based models have been shown to qualitatively reproduce the phase behavior of PEO. In this article, we will discuss the local structure of the DME/water systems in light of these models. The detailed comparison of the models with simulation of solutions of PEO chains with different degrees of polymerization (2, 3, 12, and 53 repeat units) will be presented in a future paper.

Experiment. Let us briefly review the experimental studies of DME/water and relevant PEO/water systems. There are three recent measurements[7−9] of *PVT* data for DME/water mixtures. All articles report the solution densities in the whole range of composition and in the temperature range from 263 to 353 K. They also show the dependence of excess volume V^E on composition. While the depth of the minimum in V^E differs (it varies from -2.4 to -1.7 cm^3/mol), the composition at the minimum is consistent and corresponds to the mole fraction $X_{DME} = 0.35 \pm 0.01$. Our simulations[1] yielded -1.9 cm^3/mol for the minimum in the excess volume at $X_{DME} = 0.38 \pm 0.05$.

Two studies[7,10] of the viscosity data of DME/water systems give consistent data in the whole range of compositions and temperature range of 298−318 K. It was observed that the maximum in the viscosity corresponds to $X_{DME} \approx 0.20$. The appearance of a well-defined maximum in the viscosity was explained by the supposition that some clusters or aggregates form in the system. Our simulations yield a maximum in viscosity at approximately the same composition.[1]

The measurements of the excess dielectric constant[11] also show strong deviation from ideal mixture behavior, including a maximum at $X_{DME} = 0.32$. The authors also tried to explain this behavior by formation of clusters. Very recent dielectric measurements of oligo(ethylene glycol)s−water solutions at high frequency show relaxation behavior similar to that of pure water for $X_{\text{ethylene glycol}} \leq 0.35$ and significant deviation from bulk water behavior for higher ether concentrations.[12] Ultrasonic[13] and entropy of autoionization[14] studies of this system indicated the appearance of some dynamic features around $X_{DME} = 0.18$. The appearance of extrema in solution properties as a function of composition will be discussed below in terms of the local structure in DME/water solutions.

A series of the Raman and infrared spectroscopy experiments for the DME/water and low molecular weight PEO/water systems have been made by Matsuura and co-workers.[15−18] These investigations reveal that the *tgt* conformer of DME becomes the most favorable in water solution. The reported intensity ratios of gauche and trans orientations around the C−C bond will be discussed below in our analysis of DME conformations. These studies indicated some anomalous conformational behavior of low molecular weight PEO chains in very dilute aqueous solution. The discussion of this topic is a subject of an upcoming paper.

A neutron diffraction study[19] of the PEO/water system showed that PEO chains do not perfectly fit into the bulk water structure, as was suggested by Kjellander.[4] Quasi-elastic neutron-scattering investigations[20,21] of this mixture also provide unambiguous evidence of the existence of two different kinds of water molecules in the system: "free" and "bound" to the polymer chain. A residence time of "bound" water molecules in the polymer hydration shell of about 10 ps was estimated.

Summarizing the experimental investigations of DME (PEO)/water systems, we can conclude that there are several peculiarities in the structural and dynamical behavior of these systems that might be more clearly understood by molecular dynamic simulations.

Previous Simulations. Several simulations of DME/water and PEO/water systems[22−26] have been performed. Most of these studies considered single ether molecules in aqueous solution, thereby neglecting the influence of ether−ether interactions. As the static and dynamic properties of ether/water solutions show quite strong composition dependence, ether/ether interactions may be quite important in determining solution properties. Because little attention was paid to the accuracy of the description of the conformational energetics of the ether, the ether/water interactions, and the ether/ether interactions in these studies, few definitive conclusions can be drawn from these efforts. We have demonstrated[1] that inaccurate descriptions of these interactions can result not only in quantitative differences in thermodynamic properties but even qualitative differences, such phase separation in experimentally observed miscible systems. Inconsistencies between previous simulations and experiments, that are likely due to inaccurate force fields, can be easily found. For example, in one simulation[26] it was found that the *ttg* conformer is the most probable in water solution, inconsistent with Raman[15] and IR[18] spectroscopy experiments that reveal that *tgt* is the most favorable conformer. In another study[25] the residence time of water molecules near PEO oxygen was estimated to be about 250 ps, contradicting recent QENS experiments.[21] The phase separation that we observed[1] in our simulations using a "poor" force field would not be observed in simulations involving a single ether molecule. Therefore, we have thoroughly investigated our quantum chemistry based force field by performing a series of molecular dynamic simulation of DME/water as a function of composition and by comparing of the obtained values of density, excess volume, and viscosity with experiments.[1]

Molecular Dynamics Simulations: Force Field and Methodology. A detailed description of the atomistic force field for the DME (PEO)/water systems is given in ref 1. In the current work we performed simulations using the constant temperature/pressure methods[27] implemented as described elsewhere.[28] Seven DME/water systems with mole fraction of DME X_{DME} = 0.004, 0.040, 0.100, 0.180, 0.420, 0.720, and 0.900 were

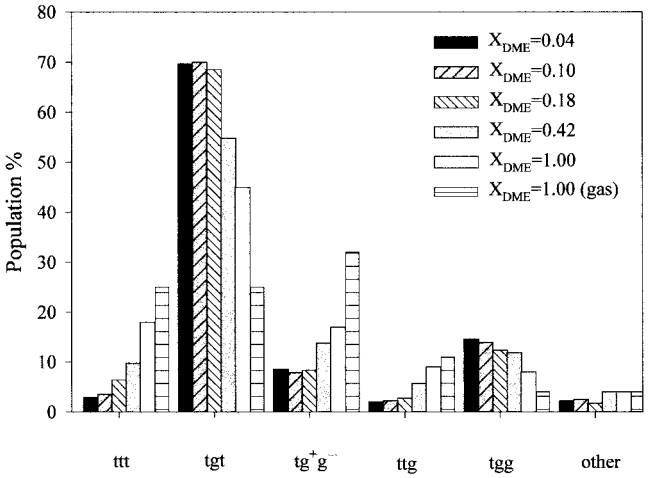

Figure 2. Composition dependence of the conformer populations for DME in aqueous solution, neat liquid, and the gas phase at 318 K.

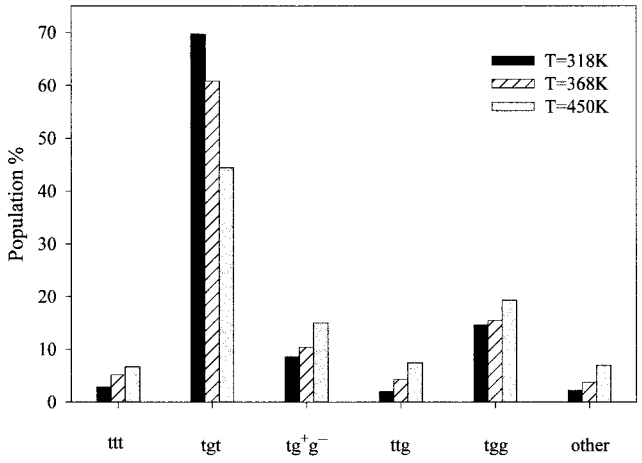

Figure 3. Temperature dependence of the conformer populations for DME in aqueous solution, $X_{DME} = 0.04$.

investigated. Simulation were performed at three different temperatures $T = 318$, 368, and 450 K and an average pressure of about 1 atm. Periodic boundary conditions were employed. The standard Shake algorithm[29] was used to constrain the bond lengths, while all other degrees of freedom remained flexible. The Ewald summation method[30] was employed to handle long-range electrostatic effects. The initial systems, consisting of DME and water molecules in a regular array with a greatly reduced density, were equilibrated for 0.1 ns. The density was increased to experimental values over 0.5 ns. Each system was then equilibrated over 2 ns. Sampling for each system occurred over 0.8 ns with a time step of 1.0 fs. Each system contained about 1300 atoms, and all systems, except $X_{DME} = 0.004$, contained at least 10 DME molecules.

III. Conformations of DME in Water

Figure 2 shows the conformer distribution of DME molecules in DME/water solutions as a function of the mole fraction of DME for $T = 318$ K. Also shown for comparison are gas-phase populations at 318 K. In the gas phase, we found that the tg^+g^- conformer is the most populous, consistent with electron diffraction experiments[31] and recent gas-phase IR investigations.[32] In the pure liquid, our simulations confirmed the strong preference of gauche conformation of the O−C−C−O bond.[33] These simulations yielded *tgt* > *ttt* > tg^+g^-, consistent with spectroscopic data for liquid DME.[34] When water is added to the liquid DME, we observe an increase in the gauche population of the O−C−C−O bond, due primarily to an increase in the *tgt* population but also the *tgg* population. It is interesting to note that for $X_{DME} \leq 0.18$ for most conformers and for $X_{DME} \leq 0.10$ for all conformers, further dilution of the system results in little change in population, consistent with the recent IR spectroscopy experiments[18] where the same saturation behavior was observed for the intensity ratio of gauche-to-trans conformations of the O−C−C−O bond. When we examine the influence of water on the population of specific conformers, we can see that the *tgt* and *tgg* populations increase significantly with increasing water content, while the *ttt*, *ttg*, and tg^+g^- populations decrease. As a result, the *tgg* conformer, the fourth most populous in pure DME liquid, is the second most populous conformer in dilute solutions. The increase in *tgg* population is consistent with recent Raman spectroscopy measurements.[35]

By comparing the populations of the various conformers as a function of temperature with those obtained from gas-phase simulations, it is possible to determine the relative free energies of interaction, or solvation, of the various conformers with water. Figure 3 shows the temperature dependence of the conformer populations for $X_{DME} = 0.04$. While the *tgt* population decreases significantly with increasing temperature, the population of each of the remaining conformers increases. Table 1 gives the relative free energies of the important conformers of DME as a function of temperature for $X_{DME} = 0.04$. At this concentration, DME interacts primarily with water. The relative (to *ttt*) conformer free energies were determined using the relationship

$$\Delta A_i = kT \ln(d_i f_{ttt}/f_i) \quad (1)$$

for each system (gas phase at $T = 318$ K and solution at each temperature). Here, i denotes a particular conformer, T is temperature, d_i is the degeneracy of the conformer (e.g., $d_{ttt} = 1$, $d_{tgg} = 4$), and f_i is the conformer population. These values are reported relative to the *ttt* conformer, as this is the lowest energy conformer in the gas phase. In solution, the *tgt* conformer has a much lower free energy than all other conformers; hence, this is the only important conformer whose population decreases with increasing temperature.

TABLE 1: Relative Free Energies of DME Conformers

	318 K		368 K		450 K		gas
	ΔA^a	$\Delta\Delta A$	ΔA	$\Delta\Delta A$	ΔA	$\Delta\Delta A$	ΔA
ttt	0.0	0.0	0.0	0.0	0.0	0.0	0.0
tgt	−1.22	−1.52	−1.29	−1.59	−1.07	−1.37	0.30
tg^+g^-	0.66	−0.04	0.51	−0.20	0.51	−0.20	0.70
tgg	0.18	−1.62	0.20	−1.60	0.29	−1.51	1.80

[a] Free energies are in kcal/mol.

The relative free energies of the DME conformers in solution are quite different from those found in the gas phase. The strength of the interaction of DME with water as a function of conformation was determined by subtracting the gas-phase values of the relative free energies (which are reasonably temperature independent) from the solution values, or

$$\Delta\Delta A_i = \Delta A_i - \Delta A_i(\text{gas phase}) \quad (2)$$

The gas-phase relative free energy differences ΔA_i(gas phase) reflect the inherent differences in energies of the conformers. Hence $\Delta\Delta A_i$ is a measure of the relative (to *ttt*) interaction of a conformer with water or the relative solvation free energies. The *tgt* and *tgg* conformers are stabilized by water (approximately −1.5 and −1.6 kcal/mol, respectively) relative to

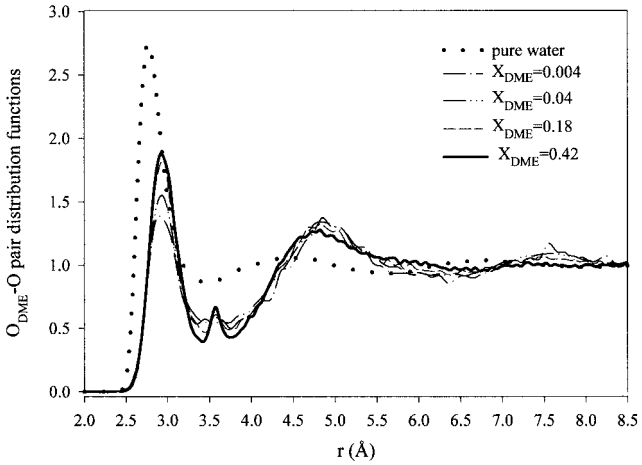

Figure 4. $O_{DME}-O$ (all) pair distribution function for various compositions of DME/water solutions at 318 K. The O_w-O_w pair distribution function for pure water is also shown.

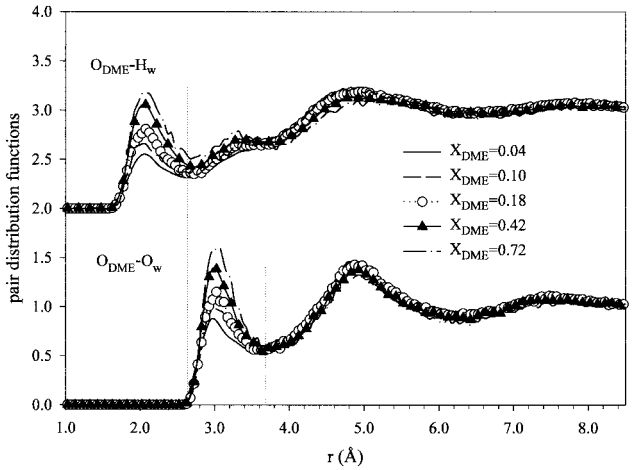

Figure 5. $O_{DME}-O_W$ and $O_{DME}-H_W$ pair distribution functions for various compositions of DME/water solutions at 318 K. Vertical lines delineate the first coordination shells.

ttt. At the same time, there is no relative stabilization of the tg^+g^- conformers.

The relative solvation energies are only weakly temperature dependent for $X_{DME} = 0.04$, indicating that they are primarily energetic (as opposed to entropic) in origin for dilute solution. However, relative solvation energies show increased temperature dependence at higher DME concentrations. To understand the large differences in the interaction of the various DME conformers with water and the influence of solution composition, we must examine the local structure in the DME/water solutions, as is done in the next section.

IV. Local Structure

The experimentally observed strong composition dependence of the static and dynamic properties of DME/water solutions and the dependence of water/DME interactions on the DME conformer seen both in our simulations and in spectroscopic measurements have led us to examine local structure in these solutions from two viewpoints. First, how does the local structure depend on the solution composition, and second, how does it depend on the DME conformer?

Composition Dependence of Local Structure. *Ether−Water Structure.* Figure 4 illustrates the pair or radial distribution function of any oxygen atom (including water, inter- and intramolecular DME oxygen atoms) around a DME oxygen atom. One reason to examine this particular pair distribution function is to check the suppositions of one of the widely discussed models of the structure of PEO/water solutions proposed by Kjellander and Florin,[4] namely that gauche positioning around the C−C bond yields $O_{DME}-O_{DME}$ distances very close to the first O−O coordination shell in pure water (2.95 and 2.85 Å, respectively). The O_{DME} atoms therefore take the position of O_w on the lattice and fit easily into the hexagonal ice structure of water. Despite the fact that Kjellander and Florin[4] consider that PEO may in fact *not* fit perfectly into the structure of water, this concept continues to form the basis of treatments of ether−water solutions (e.g., see ref 12). A recent neutron diffraction study[19] of PEO/water solutions showed that this model and other models in which PEO is supposed to fit into an unperturbed water lattice are not congruent with experimentally observed distribution of water around PEO. We reach the same conclusion from our simulations after analyzing the radial distribution functions from Figure 4. We find that even for the DME molecule, which is very short and therefore

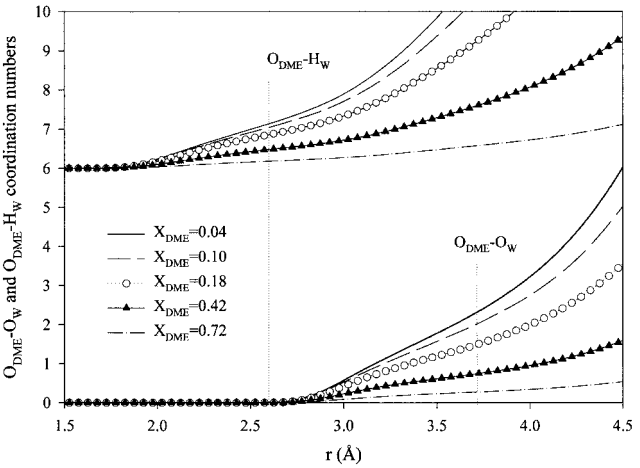

Figure 6. $O_{DME}-O_w$ and $O_{DME}-H_w$ coordination numbers for various compositions of DME/water solutions at 318 K. Vertical lines delineate the first coordination shells.

should result in relatively little disturbance in the water structure, and even for very dilute solutions, the arrangement of oxygen atoms around the DME oxygen is very different from the arrangement of water oxygen atoms in pure water.

In Figure 5, we show the $O_{DME}-O_w$ and $O_{DME}-H_w$ pair distribution functions. Figure 6 is the density weighted integral of the pair distributions in Figure 5, yielding the accumulated coordination number of water oxygen atoms or water hydrogen atoms around a DME oxygen atom. From the $O_{DME}-O_w$ pair distribution function, we can determine that the first coordination shell of water molecules around a DME oxygen atom corresponds to about 3.7 Å. Similarly, we can associate water−ether hydrogen bonds with $O_{DME}-H_w$ separations ≤ 2.6 Å. For dilute solutions, the number of hydrogen bonds per ether oxygen is slightly greater than one and the number of coordinated waters per ether oxygen is approximately two. The hydrogen bonding of water to DME shows only weak concentration dependence for dilute solutions but becomes much stronger with increasing DME concentration. The number of waters in the first coordination shell shows a greater dependence on composition. At $X_{DME} = 0.20$, there is just sufficient water for each DME oxygen to coordinate two water molecules without sharing water. $X_{DME} = 0.35$ corresponds to approximately one water molecule per ether oxygen, and Figure 6 reveals that the system has approximately one hydrogen bond per ether oxygen at this

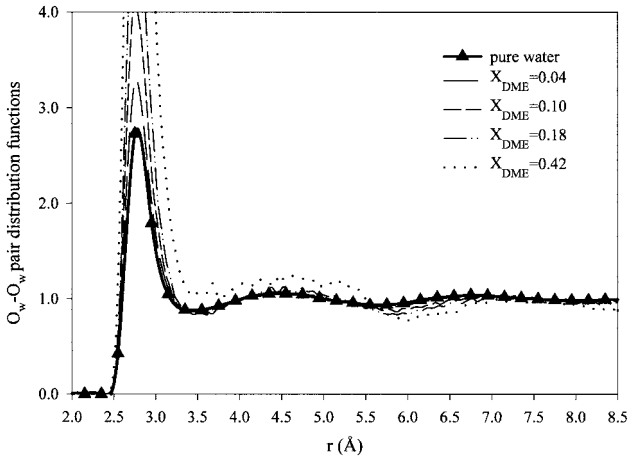

Figure 7. O_w-O_w pair distribution function for various compositions of DME/water solutions at 318 K. The O_w-O_w pair distribution function for pure water is also shown.

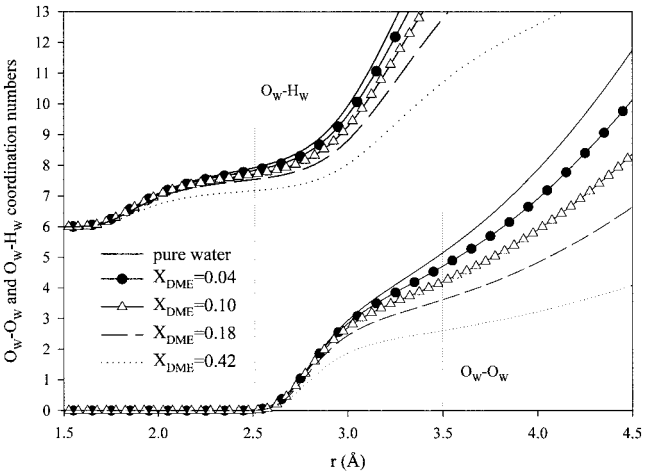

Figure 8. O_w-O_w and O_w-H_w coordination numbers for various compositions of DME/water solutions. Vertical lines delineate first coordination shells.

composition. As discussed above, many solution properties, such as the viscosity and excess volume, exhibit extrema in this composition range.

Water−Water Structure. In Figure 7 we show the O_w-O_w radial distribution functions as a function of concentration. Figure 8 illustrates the O_w-O_w coordination and O_w-H_w coordination as a function of concentration. From Figure 7, it can be seen that the longer-range (≥3.5 Å) water structure is independent of concentration for $X_{DME} \leq 0.42$, indicating solution miscibility. The number of water molecules in the first hydration shell of a given water molecule is given by Figure 8. This number is approximately 4−5 and decreases with increasing DME concentration. The number of water−water hydrogen bonds experienced by a given water molecule is about 2 and exhibits only weak dependence on composition for $X_{DME} \leq 0.18$. We can therefore conclude that for $X_{DME} \leq 0.18$ sufficient water exists in the system to allow the local water structure to resemble that in bulk water as measured by the number of water−water hydrogen bonds. At higher DME concentrations ($X_{DME} \geq 0.42$), the number of water−water hydrogen bonds becomes concentration dependent. In this concentration range, there is no longer sufficient water to complete hydrate (form hydrogen bonds with and the first coordination shell for) each DME oxygen atom. Even so, water strongly prefers to form clusters of three to four molecules as opposed to being homogeneously distributed

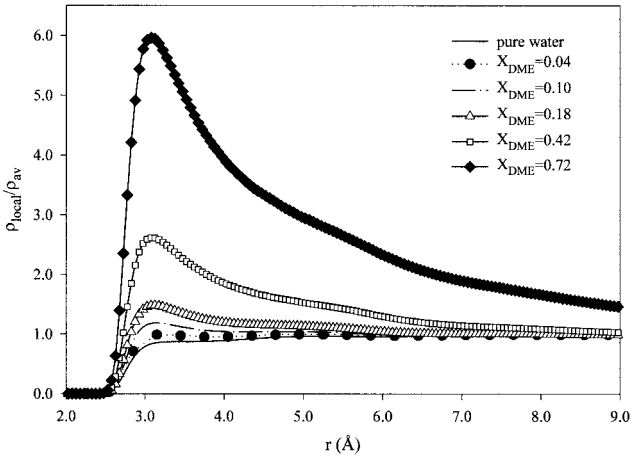

Figure 9. Ratio of the local density of water to the average density of water (see text for definitions) for various compositions of DME/water solutions at 318 K.

throughout the system, even for the lowest water concentration for ($X_{DME} = 0.90$) investigated. However, these clusters exhibit local bulklike behavior only when there is sufficient water to form approximately one $O_{DME}-H_w$ hydrogen bond per DME oxygen, indicating a competition between DME hydration and local water clustering. Behavior consistent with this picture has been observed in recent dielectric measurements[12] as discussed in the experimental review section. The local heterogeneity in the water distribution is clearly demonstrated in Figure 9, which shows the ratio of the local water density (water coordination number per unit volume in a sphere of radius r from a given water molecule) to the bulk solution density of water.

Dependence of the Local Structure on the DME Conformer. In the gas phase, strong attractive 1,5 $C(H_3)-O$ electrostatic interactions are responsible for stabilizing the tg^+g^- conformer, making this the most populous conformer.[2,36] In the liquid phase, intermolecular interactions compete with the intramolecular interactions, and as a result, the *tgt* conformer, with relatively low intrinsic energy and a large dipole moment, becomes the most populous in the polar condensed phase due to dipole−dipole interactions.[33] In aqueous solutions, hydrogen-bonding effects between water molecules and between water and DME are manifest in addition to polar interactions. These combined effects result in dramatic differences in the conformational distribution between the gas, pure liquid, and aqueous solution.

Water−DME Hydrogen Bonding. We have investigated the dependence of the local structure in DME/water solutions on the DME conformer for the *ttt*, *tgt*, *tgg*, and tg^+g^- conformers. The $O_{DME}-O_w$ radial distribution functions for each conformer are shown in Figure 10 for dilute solution ($X_{DME} = 0.04$) at temperature $T = 318$ K. Surprisingly, these functions are quite similar, indicating that the distribution of water around the conformer does not depend strongly on the particular conformer. The first peak, at around 3 Å, corresponds to water molecules that form hydrogen bonds with DME oxygen atoms. The extent of hydrogen bonding is nearly independent of the DME conformer. The energetics of forming hydrogen bonds with the ether oxygen atoms are overwhelmingly favorable, and these bonds form regardless of the ether conformation. Hence, the supposition that the *tgt* conformer is stabilized in water (relative to other conformers) because its geometry is more compatible with the liquid water structure is incorrect.[4,12,15] This conclusion is further reinforced by Figure 11, which compares the O_w-

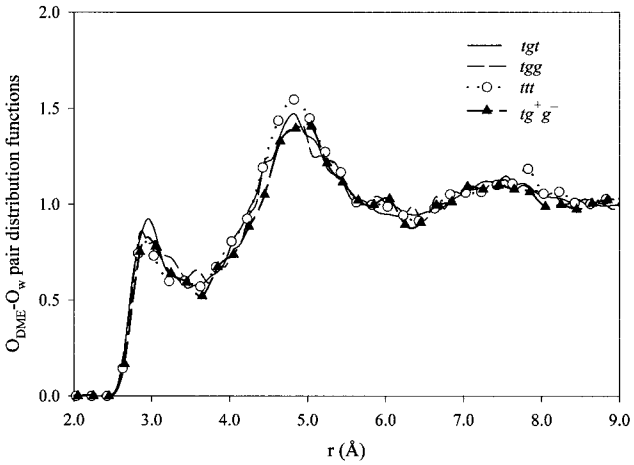

Figure 10. $O_{DME}-O_w$ pair distribution function for various DME conformers in $X_{DME} = 0.04$ DME/water solution at 318 K.

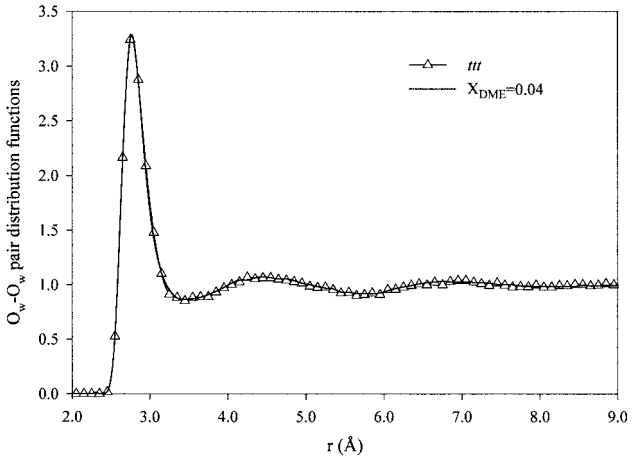

Figure 11. O_w-O_w pair distribution function for various DME conformers in $X_{DME} = 0.04$ DME/water solution at 318 K.

O_w pair distribution function for a composition of $X_{DME} = 0.04$, where the DME is primarily in the *tgt* conformer, with that for a simulation at the same composition where the DME is constrained to the *ttt* conformer. The water structure is independent of the DME conformer (for dilute solutions).

Stabilization in Dilute Solution. The relative stabilization of the *tgt* and *tgg* conformers (see Table 1) in dilute aqueous solution is not due to their specific geometry that allows them to fit perfectly into the water structure or form more hydrogen bonds with water than other conformers. Hence, some other factor is responsible for this stabilization. That this stabilization is at least partially energetic in origin is supported by the fact that the difference in total energy of an $X_{DME} = 0.04$ solution at 318 K, where the DME is primarily *tgt*, is 1.4 kcal/mol per DME molecule lower than for the simulation with constrained *ttt* DME. This number is in excellent agreement with the ΔA value in Table 1 for *tgt* obtained from the temperature dependence of the conformer populations in dilute solutions. Subtracting the 0.1 kcal/mol inherent energy for *tgt* yields a $\Delta\Delta A$ of −1.5 kcal/mol, again in good agreement with Table 1.

From the simulation trajectories we determined the total energy of interaction of DME in various conformations with the waters in the vicinity of 7.5 Å (first and second ether oxygen hydration shells) from the center of the C−C bond. We divided this energy in two contributions, the DME−water interaction and water−water interaction for these neighboring waters. These calculations show that, for the *tgt* and *tgg* conformers,

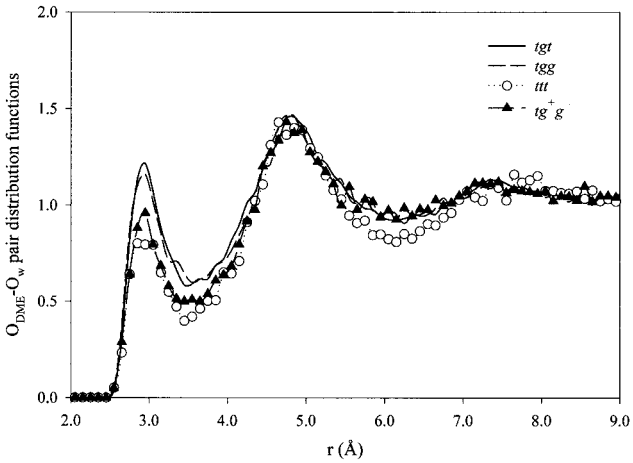

Figure 12. $O_{DME}-O_w$ pair distribution function for various DME conformers in $X_{DME} = 0.18$ DME/water solution at 318 K.

the DME−water interactions are approximately 2.5 kcal/mol more favorable than for the *ttt* conformer. At the same time the water−water interaction for waters in the neighborhood of the *tgt* and *tgg* conformers is less favorable by about 1.0 kcal/mol relative to *ttt*. For the tg^+g^- conformer the DME−water and water−water interactions are roughly equal in magnitude, with the former being favorable by 1.0 kcal/mol and the latter unfavorable by the same energy.

Because of polar nature of the water, it is obvious that, as in DME liquid, conformers with relatively high dipole moments should be stabilized in aqueous solution relative to nonpolar conformers. Polar interactions should stabilize the *tgt*, tg^+g^-, and *tgg* conformers, with large dipole moments[33] (1.7, 1.6, and 2.9 D, respectively), in aqueous solution relative to the *ttt* conformer, which has a zero dipole moment**.** This is consistent with the values of DME−water interactions given above. However, the tg^+g^- conformer, which has approximately the same dipole moment as the *tgt* conformer, has a significantly less favorable interaction with water. The positioning of the waters that are hydrogen bound to the tg^+g^- conformer results in relatively unfavorable dipole−dipole orientation not only between these waters and the DME molecule but also between DME and the neighboring waters which are highly correlated with the bound waters. Competing DME−water and water−water polar interactions result in less favorable polar interactions between water neighboring all polar conformers when compared to the nonpolar *ttt* conformer. The competition of these effects is responsible for the relative stabilization of particular conformers. To summarize, as hydrogen bonding is approximately equal for all conformers, the relative stabilization of the *tgt* and *tgg* conformers is due to the fact that their dipole moments are more favorably aligned with the local water structure than that of the tg^+g^- conformer.

Concentration Dependence. Correlation between composition and conformation dependence of the local structure was found when we analyzed the $O_{DME}-O_w$ and the intermolecular $O_{DME}-O_{DME}$ radial distribution functions for different conformers for $X_{DME} = 0.18$ at temperature $T = 318$ K. The $O_{DME}-O_w$ pair distribution function is illustrated in Figure 12. This figure can be compared with results for $X_{DME} = 0.04$ in Figure 10. Unlike the more dilute case, the $O_{DME}-O_w$ distribution for $X_{DME} = 0.18$ is dependent upon the conformer, especially in the first coordination shell. There is no difference between these functions for the "hydrophilic" *tgt* and *tgg* conformers, while these functions for the "hydrophobic" *ttt* and tg^+g^- conformers are noticeably different from these. If we look at the distance

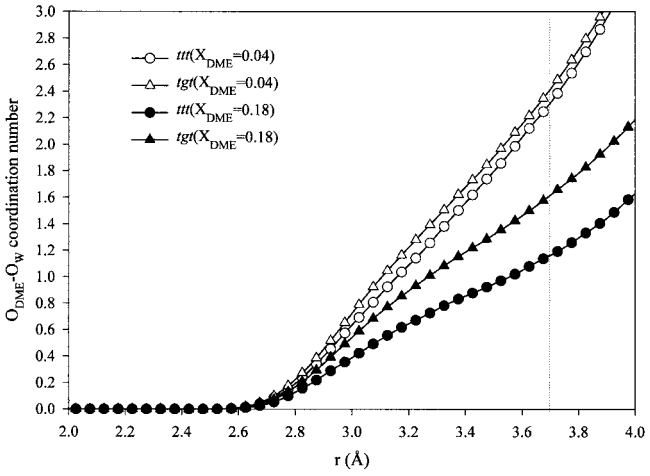

Figure 13. $O_{DME}-O_w$ coordination number for *tgt* and *ttt* conformers at $X_{DME} = 0.04$ and 0.18 in DME/water solutions at 318 K. Vertical line delineates the first coordination shell.

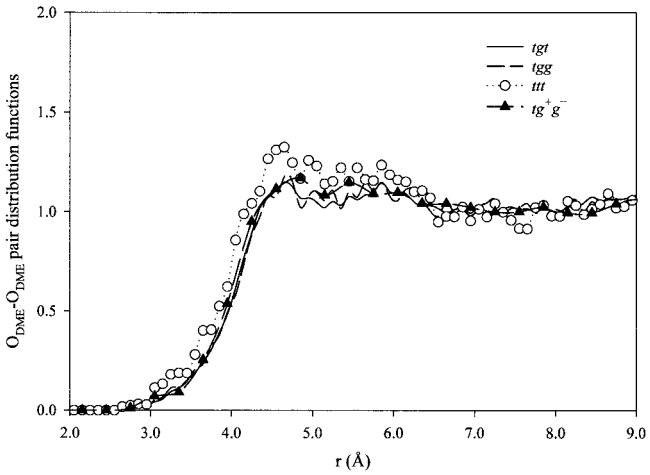

Figure 14. $O_{DME}-O_{DME}$ pair distribution function for various DME conformers in $X_{DME} = 0.18$ DME/water solution at 318 K.

dependence of the number of water molecules around the O_{DME} in a sphere of radius *r* (Figure 13), we also see a concentration dependence that is a function of the conformer. For $X_{DME} = 0.04$ the number of water molecules in the radius of 3.7 Å (first coordination shell) for the *ttt* conformer is almost the same as for the *tgt* conformer, while the *tgt* conformer has a definite preference for water compared to *ttt* for $X_{DME} = 0.18$. These effects can be further understood by analysis of the intermolecular $O_{DME}-O_{DME}$ radial distribution functions for different conformers at $X_{DME} = 0.18$. These are shown in the Figure 14. Unlike the case for $X_{DME} = 0.04$ (not shown), where the intermolecular $O_{DME}-O_{DME}$ pair distribution functions were found to be independent of the conformer**,** the *ttt* conformer is more likely to have another DME molecule in the close vicinity than other (*tgt* and *tgg*) conformers.

Analysis of this behavior may lead to some insight into the phase behavior of PEO/water solutions. At higher DME concentrations there is a tendency for hydrophobic DME conformers (e.g., *ttt* and tg^+g^-) to interact, while hydrophilic conformers (*tgt* and *tgg*) still prefer to be surrounded by water. This explains why the *ttt* and tg^+g^- conformers have relatively few water molecules as neighbors at the higher DME concentration in comparison with *tgt* and *tgg* conformers. At higher DME concentrations, analysis of the temperature dependence of the conformer populations reveals that, unlike dilute solutions, the relative (to *ttt*) free energies of solvation are temperature dependent for hydrophilic conformers, indicating relatively unfavorable entropic contributions to the solvation of hydrophilic conformers in the nondilute solutions. The following picture of DME solvation emerges. For dilute solutions, addition of a DME molecule results in hydrogen bonding between DME and water. At the same time, the extent of hydrogen bonding in the water remains constant, resulting in increased local water structure and decreased entropy. These effects do not depend strongly on the DME conformer, and the greater preference for hydrophilic conformers is primarily a result of favorable polar interactions between DME and water. Hence, differences in the relative free energies of solvation for the various conformers in dilute solution are mostly energetic in origin. When a DME molecule is added to a solution of higher DME concentration, the molecule can also interact with other DME molecules. When the DME is in a hydrophobic conformer, it will on average interact with more DME molecules and fewer water molecules than a hydrophilic conformer. As a result, the hydrophobic conformer has a smaller influence on the water structure and hence is entropically favored but energetically penalized (fewer hydrogen bonds with water) relative to the hydrophilic conformers. With increasing temperature, these energetic and entropic effects will increasingly favor hydrophobic conformers and hence may lead to the LCST observed in PEO/water solutions. This question will be discussed in more detail in our upcoming papers.

V. Conclusions

Through analysis of the composition and conformation dependence of the local structure in DME/water solutions, it is shown that DME does not fit into the water oxygen network as is suggested by Kjellander and Florin.[4] At the same time, the local structure of water around the ether, including the extent of hydrogen bonding, does not depend strongly on the conformational geometry of the DME for dilute solution. Hence, the model of Goldstein,[5] which supposes forms of PEO that form hydrogen bonds with water and forms that do not, appears to be an incorrect, at least for dilute solutions. The relative stabilization of the different conformers can be explained by differences in *polar* interactions. All polar conformers have favorable polar interactions with water that result in unfavorable water−water polar interactions, relative to those for water surrounding the nonpolar *ttt* conformer. For the *tgt* and *tgg* conformers, the net dipolar interaction (DME−water + water−water) is relatively favorable, and these hydrophilic conformers are stabilized in aqueous solution. The nonpolar *ttt* and the polar tg^+g^- conformers are relatively hydrophobic, the latter due to unfavorable net dipolar interactions. This behavior is consistent with the model of Karlstom,[5] which supposes a polar "low-temperature" and a nonpolar "high-temperature" form of PEO. Finally, our simulations indicate that entropic effects, resulting from increased local water structure in the presence of DME, are important in determining conformations in nondilute DME/water solutions. Both entropic and energetic effects may therefore be responsible for the phase behavior of PEO/water solutions. Hence, the theoretical models, which consider either entropic[4] *or* energetic[5,6] effects, but not both, are incomplete.

Acknowledgment. The authors are indebted to the National Science Foundation-Division of Materials Research for support provided through Grant NSF DMR 9624475.

References and Notes

(1) Bedrov, D.; Pekny, M.; Smith, G. D. *J. Phys. Chem. B* **1998**, *102*, 996.

(2) Jaffe, R. L.; Smith, G. D.; Yoon, D. Y. *J. Phys. Chem.* **1993**, *97*, 12752.

(3) Jorgensen, W. L.; Chandrasekhar, J.; Madura, J. D.; Impey, R. W.; Klein, M. *J. Chem. Phys.* **1983**, *79*, 926.

(4) Kjellander, R.; Florin, E. J. *J. Chem. Soc., Faraday Trans. 1* **1981**, *77*, 2053.

(5) Goldstein, R. E. *J. Chem. Phys.* **1984**, *80*, 5340.

(6) Karlstrom, G. *J. Phys. Chem.* **1985**, *89*, 4962.

(7) Das, B.; Roy, M. N.; Hazra, D. K. *Indian J. Chem. Technol.* **1994**, *1*, 93.

(8) Marchetti, A.; Tassi, L.; Ulrici, A. *Bull. Chem. Soc. Jpn.* **1997**, *70*, 987.

(9) Douheret, G.; Davis, M. I.; Hernandez, M. E.; Flores, H. *J. Indian. Chem. Soc.* **1993**, *70*, 395.

(10) Ramanamurti, M. V.; Prabhu, P. V. S. S.; Bahadur, S. L. *Bull. Chem. Soc. Jpn.* **1986**, *59*, 2341.

(11) Prabhu, P. V. S. S.; Ramanamurti, M. V. *Bull. Chem. Soc. Jpn.* **1992**, *65*, 1716.

(12) Sato, T.; Niwa, H.; Chiba, A.; Nozaki, R. *J. Chem. Phys.* **1998**, *108*, 4138.

(13) Takenaka, N.; Arakawa, K. *Bull. Chem. Soc. Jpn.* **1974**, *47*, 566.

(14) Datta, J.; Kundu, K. *Can. J. Chem.* **1981**, *59*, 3141.

(15) Yoshida, H.; Takikawa, K.; Kaneko, I.; Matsuura, H. *THEOCHEM* **1994**, *311*, 205.

(16) Masatoki, S.; Takamura, M.; Matsuura, H.; Kamogawa, K.; Kitagawa, T. *Chem. Lett.* **1995**, 991.

(17) Matsuura, H.; Sagawa, T. *J. Mol. Liq.* **1995**, *65/66*, 313.

(18) Begum, R.; Matsuura, H. *J. Chem. Soc., Faraday Trans.* **1997**, *93*, 3839.

(19) Bieze, T. W. N.; Barnes, A. C.; Huige, C. J. M.; Enderby, J. E.; Leyte, J. C. *J. Phys. Chem.* **1994**, *98*, 6568.

(20) Crupi, V.; Jannelli, M. P.; Magazu, S.; Maisano, G.; Majolino, D.; Migliardo, P.; Vasi, C. *Il Nuovo Cimento* **1994**, *16D*, 809.

(21) Barnes, A. C.; Bieze, T. W. N.; Enderby, J. E.; Leyte, J. C. *J. Phys. Chem.* **1994**, *98*, 11527.

(22) Liu, H.; Muller-Plathe, F.; van Gunsteren, W. F. *J. Chem. Phys.* **1995**, *102*, 1722.

(23) Engkvist O.; Astrand, P.; Karlstrom, G. *J. Chem. Phys.* **1996**, *100*, 6950.

(24) Williams, D. J.; Hall, K. B. *J. Phys. Chem.* **1996**, *100*, 8224.

(25) Tasaki, K. *J. Am. Chem. Soc.* **1996**, *118*, 8459.

(26) Engkvist O.; Karlstrom, G. *J. Chem. Phys.* **1997**, *106*, 2411.

(27) Nose, S. *J. Chem. Phys.* **1984**, *81*, 511.

(28) Smith, G. D.; Jaffe, R. L.; Yoon, D. Y. *Macromolecules* **1993**, *26*, 298.

(29) Ryckaert, J.; Ciccotti, G.; Berendsen, H. J. C. *J. Comput. Phys.* **1977**, *23*, 327.

(30) Allen, M. P.; Tildesley, D. T. *Computer Simulation of Liquids*; Oxford: New York, 1987.

(31) Astrup, F. E. *Acta Chem. Scand.* **1979**, *A33*, 655.

(32) Yoshida, H.; Tanaka, T.; Matsuura, H. *Chem. Lett.* **1996**, *8*, 637.

(33) Smith, G. D.; Jaffe, R. L.; Yoon, D. Y. *J. Am. Chem. Soc.* **1995**, *117*, 530.

(34) Ogawa, Y.; Ohta, M.; Sakakibara, M.; Matsuura, H.; Harada, I.; Shimanouchi, T. *Bull. Chem. Soc. Jpn.* **1977**, *50*, 650.

(35) Yoshida, H.; Matsuura, H. *J. Phys. Chem. A* **1998**, *102*, 2691.

(36) Jaffe, R. L.; Smith, G. D.; Yoon, D. Y. *J. Phys. Chem.* **1993**, *97*, 12745.